AIP | Applied Physics Letters

Interactions of defect complexes and domain walls in CuO-doped ferroelectric (K,Na)NbO3

Rüdiger-A. Eichel, Ebru Erünal, Peter Jakes, Sabine Körbel, Christian Elsässer et al.

Citation: Appl. Phys. Lett. **102**, 242908 (2013); doi: 10.1063/1.4811268
View online: http://dx.doi.org/10.1063/1.4811268
View Table of Contents: http://apl.aip.org/resource/1/APPLAB/v102/i24
Published by the AIP Publishing LLC.

Interactions of defect complexes and domain walls in CuO-doped ferroelectric (K,Na)NbO_3

Rüdiger-A. Eichel,[1,a)] Ebru Erünal,[2] Peter Jakes,[1] Sabine Körbel,[3] Christian Elsässer,[3] Hans Kungl,[1,4] Jérôme Acker,[4,b)] and Michael J. Hoffmann[4]
[1]*Forschungszentrum Jülich, Institut für Energie- und Klimaforschung (IEK-9), D-52425 Jülich, Germany*
[2]*Institut für Physikalische Chemie, Universität Freiburg, Albertstr. 21, D-79104 Freiburg, Germany*
[3]*Fraunhofer-Institut für Werkstoffmechanik IWM, Wöhlerstr. 11, D-79108 Freiburg, Germany*
[4]*Karlsruher Institut für Technologie (KIT), Institut für Angewandte Materialien-Keramik im Maschinenbau (IAM-KM), D-76131 Karlsruhe, Germany*

(Received 17 March 2013; accepted 30 May 2013; published online 19 June 2013)

"Lead-free" piezoelectric sodium potassium niobate has been studied with respect to its defect structure when doping with CuO. The results indicate that two kinds of mutually compensating charged defect complexes are formed, $(Cu''''_{Nb} - V^{\bullet\bullet}_O)'$ and $(V^{\bullet\bullet}_O - Cu''''_{Nb} - V^{\bullet\bullet}_O)^{\bullet}$. Concerning the interplay of these defect complexes with the piezoelectric materials properties, the trimeric $(V^{\bullet\bullet}_O - Cu''''_{Nb} - V^{\bullet\bullet}_O)^{\bullet}$ defect complex primarily has an elastic dipole moment and thus is proposed to impact the electromechanical properties, whereas the dimeric $(Cu''''_{Nb} - V^{\bullet\bullet}_O)'$ defect possesses an electric dipole moment in addition to an elastic distortion. Both types of defect complexes can impede domain-wall motion and may contribute to ferroelectric "*hardening*." © *2013 AIP Publishing LLC*. [http://dx.doi.org/10.1063/1.4811268]

Point defects and defect complexes play an important role to tailor functional materials. In ferroelectrics, which allow to convert mechanical to electrical energy and vice-versa, for applications ranging from medical imaging to non-volatile memories, electro-mechanical sensors, transducers or actuators, "*hard*" or "*soft*" behavior critically depends on the nature of point defects. Particularly dimeric defect complexes between acceptor-type dopant ions and charge-compensating oxygen vacancies have pronounced impact on the properties of these materials. By exploiting the electric and elastic properties associated with these defect dipoles,[1] their interaction with the domain structure and domain walls is discussed in terms of materials hardening,[1] aging,[1,2] and electrical fatigue.[3,4] It has been shown recently for Mn-doped barium titanate single crystals that the behavior of dimeric $(Mn''_{Ti} - V^{\bullet\bullet}_O)^{\times}$ defect dipoles explains the underlying mechanism of high electro-mechanical strain in terms of a symmetry-conforming short-range ordering principle between defect complexes and ferroelectric domains.[2]

Motivated by environmental concerns because of the toxicity of lead oxide current research focuses on the search for "*lead-free*" alternatives to the widely used $Pb[Zr_{1-x}Ti_x]O_3$ (PZT) solid-solution system which show comparable performance.[5–8] Promising alternatives are modified alkali niobates ($[K_yNa_{1-y}]NbO_3$, KNN) and solid solutions between bismuth sodium titanate and barium titanate (BNT-BT) with a composition close to a morphotropic phase boundary.[9,10] KNN ceramics modified with Li, Ta, or Sb have been reported to exhibit suitable piezoelectric properties for actuator applications at ambient temperature.[11] However, the main difference between PZT and lead-free ferroelectrics manifests itself in the fact that PZT with small chemical modifications is a robust multi-purpose piezoelectric material, whereas for the presently known lead-free compounds variations in composition are mandatory to tailor properties for specific applications.[8]

In respect to the defect structure, the mechanisms of charge compensation when considering acceptor doping with aliovalent ions on perovskite B-sites are expected to considerably differ between PZT, BNT-BT, and KNN. Whereas in the two former cases the B-site ion is tetravalent (Ti^{4+}, Zr^{4+}), for KNN it is pentavalent (Nb^{5+}). As consequence the investigated mechanism of compensating the excess charge associated with an Cu^{2+}-acceptor dopant with one oxygen vacancy by formation of a charge neutral $(Cu''_{Ti} - V^{\bullet\bullet}_O)^{\times}$ defect complex,[12] cannot directly be transferred to Cu^{2+}-doped KNN. It is hence of significant interest to understand the origin of modified materials properties on an atomic scale. Concerning CuO-doped KNN, an enhanced mechanical quality factor Q_m and a hardening has recently been reported,[13–15] whereby the question has remained unanswered what is the kind of defect structure and how this impacts the domain structure.

KNN 50/50 containing 0.25 mol. % Cu, $(K_{0.5}Na_{0.5})(Nb_{0.9975}Cu_{0.0025})O_{2.99625}$, was prepared by a mixed oxide-carbonate route.[35,36] K_2CO_3, Na_2CO_3, Nb_2O_5, and CuO were mixed by attrition milling in isopropanol, dried, sieved, and calcined at 775 °C for 5 h. After final ball milling, drying and sieving, pellets were formed by uniaxial and cold isostatic pressing at 500 MPa. Sintering at 1105 °C for 2 h resulted in ceramics with 4.3 g cm^{-3} density. All peaks in the XRD patterns of the KNN-0.25 Cu ceramics recorded with a Siemens D500 diffractometer with Cu-K_α radiation ($\lambda = 1.5406$ Å) could be attributed to the perovskite type orthorhombic $KNbO_3$ structure (cf., Figure 1(a)). No secondary phases were detected by the X-ray at the low level of Cu-doping. The microstructure of the KNN-Cu ceramics, observed by SEM (Leica Stereoscan 440) of polished and chemically (H_2O-HCl-HF solution) etched surfaces, as depicted in

a)Author to whom correspondence should be addressed. Electronic mail: r.eichel@fz-juelich.de
b)Present address: Continental Automotive GmbH, Siemensstraße 12, D-93055 Regensburg, Germany.

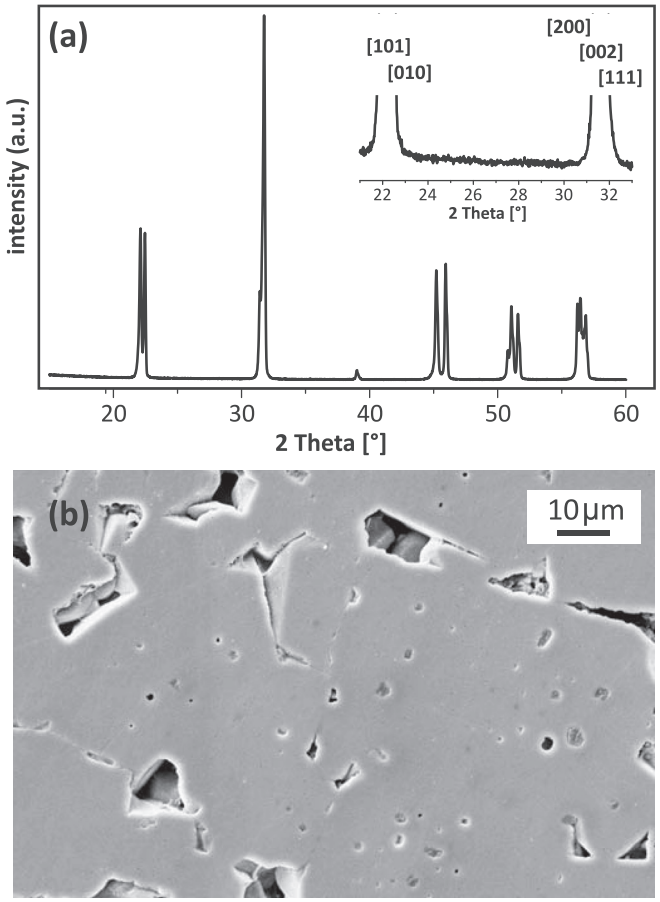

FIG. 1. Structure and microstructure of 0.25 mol. % Cu-doped KNN 50/50 ceramics. (a) XRD pattern. The inset shows the region where secondary phases would be expected with enhanced magnification. Peaks are indexed according to JCPDS 71-2171. (b) SEM micrograph of the polished and chemically etched surface.

Figure 1(b), showed large grains with non-polyhedral shapes and sizes ranging between 30 and 50 μm. Most marked there is a considerable amount of intragranular porosity present in many of the grains.[35,36]

First-principles calculations using Density-functional theory (DFT) in the local-density approximation (LDA) were performed to calculate the defect formation energies of V_O, $(Cu_{Nb} - V_O)$ and $(V_O - Cu_{Nb} - V_O)$ in cubic KNN 50/50. The defect formation energies were calculated for different charge states and as a function of the Fermi energy (the chemical potential of the electrons). A compensating homogeneous background charge was included in the supercell calculation of electrostatic energies and potentials. The binding energies of the defect complexes were calculated as differences between the formation energy of the complexes and the sum of the formation energies of the isolated defects. The formalism applied is related to that of Ref. 37. The total energies of the defect complexes were calculated for atomistic supercell models containing $2 \times 2 \times 3$ perovskite unit cells. The computational mixed-basis pseudopotential methodology[38,39] was the same as that employed in the preceding studies of doped $KNbO_3$ and KNN[18] (more details are given there). The mixed perovskite KNN was modelled with a Virtual Crystal Approximation[40,41] for the alkaline atoms.

Electron paramagnetic resonance (EPR) measurements were performed on a Q-band (34.1 GHz) Bruker ESP 380 spectrometer in a temperature interval between 20 K and ambient temperature. The used spin Hamiltonian for an unpaired $3d^9$ electron with spin $S = \frac{1}{2}$ is

$$\mathcal{H} = \beta_e \mathbf{B_0} \cdot \mathbf{g} \cdot \mathbf{S} - \beta_n g_n \mathbf{B_0} \cdot \mathbf{I} + \mathbf{S} \cdot \mathbf{A} \cdot \mathbf{I}, \quad (1)$$

where g_n is the nuclear g-factor and β_e and β_n are the Bohr and nuclear magnetons, respectively. The first and second terms represent the electronic and nuclear Zeeman interactions, respectively, where $\mathbf{B_0}$ denotes the external field, given in the principal axes system of the $\mathbf{g}$-matrix. The last term is due to the copper hyperfine interaction with $I^{Cu} = \frac{3}{2}$ for both copper isotopes with natural abundances ^{63}Cu (69.09%) and ^{65}Cu (30.91%).

DFT and electron paramagnetic resonance (EPR) spectroscopy have been combined in order to approach these types of questions before.[16,17] In a previous DFT study,[18] it was found that in thermal equilibrium at ambient pressure and temperature Cu substitutionals in KNN are more stable on Nb than on alkali sites. In this DFT study, we therefore assume that Cu substitutes on Nb sites. Assuming that oxygen vacancies are abundant, the concentration ratio of $(Cu_{Nb} - V_O)$ and $(V_O - Cu_{Nb} - V_O)$ is determined by their respective binding energies. In the present study, we compare $(Cu_{Nb} - V_O)$ and a linear configuration of $(V_O - Cu_{Nb} - V_O)$ in which the V_O are located on opposite sides of the Cu_{Nb}-substitutional. However, other defect configurations such as $(Cu_A - V_A)$ or an angular $(V_O - Cu_{Nb} - V_O)$ defect complex are not ruled out by present DFT results. They will be discussed elsewhere.[19,20]

Figure 2 shows the corresponding binding energies of $(Cu_{Nb} - V_O)$ and $(V_O - Cu_{Nb} - V_O)$ as function of the Fermi level as obtained with DFT. Over the entire theoretical band gap, the binding energies are negative (between -0.8 and -2.4 eV), indicating stable defect complexes with respect to isolated Cu_{Nb} and V_O.

Although the $(V_O - Cu_{Nb} - V_O)$ complex is energetically more favorable, both types of defect complexes may exist at finite temperatures because $(Cu_{Nb} - V_O)$ and an isolated oxygen vacancy have a higher configurational entropy than $(V_O - Cu_{Nb} - V_O)$.

Experimentally, the anticipated defect structure has been probed by EPR. The corresponding Q-band (34.1 GHz) EPR spectrum of copper-doped KNN is shown in Fig. 3. It

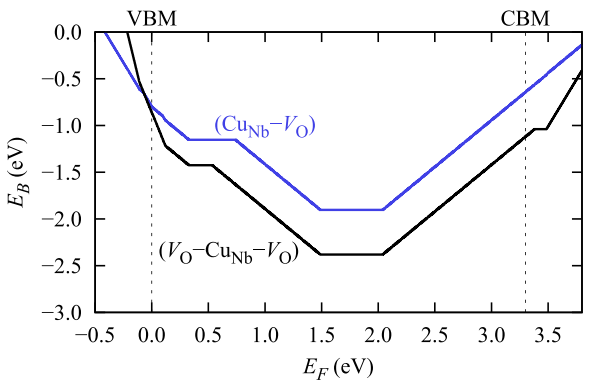

FIG. 2. Binding energies of the defect complexes $(Cu_{Nb} - V_O)$ and $(V_O - Cu_{Nb} - V_O)$ vs. Fermi energy calculated with DFT. VBM and CBM denote the valence band maximum and conduction band minimum, respectively.

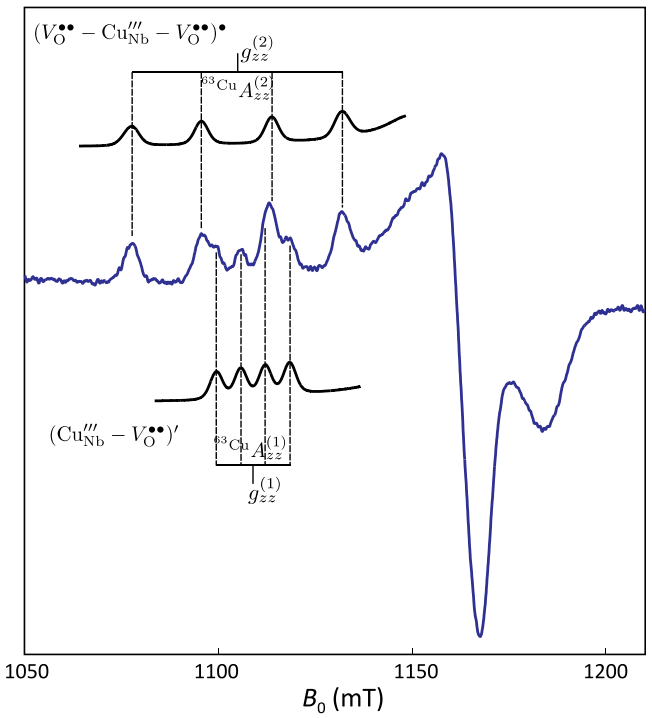

FIG. 3. Q-band (34.1 GHz) EPR-spectrum of a 0.25 mol. % copper-doped KNN 50/50 ceramic, recorded at a temperature of 20 K. The two different quartet hyperfine structures for two different types of Cu^{2+} centers are indicated. The two observed centers indicate the formation of mutually compensating $(Cu_{Nb}''' - V_O^{\bullet\bullet})'$ and $(V_O^{\bullet\bullet} - Cu_{Nb}''' - V_O^{\bullet\bullet})^{\bullet}$ defect complexes.

consists of two superimposed subspectra that both are characteristic for $S = \frac{1}{2}$ systems with hyperfine coupling to a nucleus of $I = \frac{3}{2}$, indicating charge states of Cu^{2+} ($3d^9$). The low-field region shows two sets of markedly different quartet hyperfine patterns ($A_{zz}^{(1,2)}$) that are centered at slightly different g-values ($g_{zz}^{(1,2)}$). The quartet hyperfine structure is due to copper nuclei with $I = \frac{3}{2}$ in different oxygen coordinations, since the EPR spin-Hamiltonian parameters in first approximation are influenced by the first coordination sphere of the Cu^{2+} functional centers.

Taking into account that $g_{zz} > g_{yy}, g_{xx}$, with approximately $g_{zz} \approx 2.2(0)$ and $g_{yy}, g_{xx} \approx 2.08(5)$ for both centers, the Cu^{2+}-site has to be octahedrally coordinated, which corresponds to the perovskite B-site and is consistent with recent results obtained by DFT calculations.[18] The corresponding size of the ionic radii, $r_{Nb^{5+}} = 64$ pm and $r_{Cu^{2+}} = 73$ pm as compared to $r_{K^+} = 164$ pm and $r_{Na^+} = 139$ pm, support this assignment.

The determined set of spin-Hamiltonian parameters ($g_{zz}^{(1)} = 2.197, {}^{63}Cu A_{zz}^{(1)} = 190$ MHz) and ($g_{zz}^{(2)} = 2.205, {}^{63}Cu A_{zz}^{(2)} = 550$ MHz) for the two copper centers can be transferred into structural information according to a recently developed semi-empirical scheme.[21] The result is in line with the theoretically anticipated defect structure that consists of two different kinds of charged defect complexes. In the first complex, $(Cu_{Nb}''' - V_O^{\bullet\bullet})'$, Cu_{Nb}''' is partially charge compensated by one oxygen vacancy. Consequently, this defect complex contains an *electric dipole* moment resulting from the charges $q = +2e$ at the oxygen vacancy site and $q = -3e$ at the Cu^{2+} site, separated by a distance of about half a lattice constant, $r_{Cu_{Nb}'''-V_O^{\bullet\bullet}} \approx 2$ Å.

In the second complex, $(V_O^{\bullet\bullet} - Cu_{Nb}''' - V_O^{\bullet\bullet})^{\bullet}$, Cu_{Nb}''' is electrically overcompensated by two oxygen vacancies.

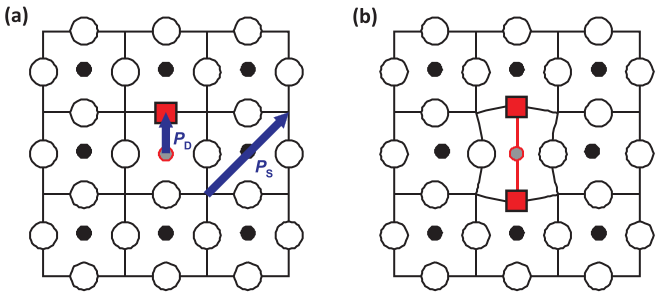

FIG. 4. $(Cu_{Nb}''' - V_O^{\bullet\bullet})'$ and $(V_O^{\bullet\bullet} - Cu_{Nb}''' - V_O^{\bullet\bullet})^{\bullet}$ defect complexes, showing only the B-sites (solid circles) and the oxygen (open circles) ions, as well as oxygen vacancies (red squares). (a) Electric dipole with indicated orientations for spontaneous (P_S) and defect polarization (P_D). (b) Elastic dipole with anticipated lattice deformation.

Owing to the Jahn-Teller effect for Cu^{2+} centers, the "equatorial" oxygen ions will presumably be rather strongly bound, whereas the "apical" oxygen ions are more weakly bound, determining the preferred position for oxygen vacancies, such that the defect complex is approximately inversion symmetric and does not have an electrical dipole moment. This assignment is supported by the observed almost axial symmetry of the spin-Hamiltonian g-matrix ($g_{xx}^{(2)} \approx g_{yy}^{(2)}$). On the other hand, both the two $V_O^{\bullet\bullet}$ and the Cu^{2+} will deform the lattice to some extent, which may be described in terms of an *elastic dipole* moment. With DFT an elongation of the Cu-Nb distances along the defect axis by 4% was obtained.

Schematically, the proposed defect structure is illustrated in Figure 4, where for simplicity a quasi-cubic crystal symmetry was chosen. This simplification is justified, because most recently it has been demonstrated that the interaction of defect complexes with domain structure in terms of the symmetry-conforming short-range ordering principle is valid for tetragonal, rhombohedral, or orthorhombic crystal symmetry.[22] Correspondingly, the deviation between the coordinate systems for defect (P_D) and spontaneous polarization (P_S) for non-axial crystal symmetries may be neglected in first approximation. Deviations from the experimentally observed axial symmetry of the defect complexes are typically observed either if the crystal symmetry of the host lattice is lower than axial,[23] if the defect complexes have their main axis along a different orientation than the direction of spontaneous polarization,[24] or if the defect complexes are located near domain walls;[25] a situation that is not observed here.

A particular feature of EPR spectroscopy is its ability to provide quantitative information in order to formulate defect chemical equations.[26–28] By analyzing the EPR spectra quantitatively, we obtain about equal concentrations of the two defect complexes, so that the two kinds of defect complexes *mutually compensate* each other, according to the electroneutrality condition,[29]

$$[(Cu_{Nb}''' - V_O^{\bullet\bullet})'] \approx [(V_O^{\bullet\bullet} - Cu_{Nb}''' - V_O^{\bullet\bullet})^{\bullet}]. \quad (2)$$

Correspondingly, each Cu^{2+}-center is charge compensated on average by $\frac{3}{2} V_O^{\bullet\bullet}$ by the formation of the two type of defect complexes according to the following incorporation reaction:

$$K_2CO_3 + Na_2CO_3 + Nb_2O_5 + 2CuO \xrightarrow{KNN} (V_O^{\bullet\bullet} - Cu_{Nb}''' - V_O^{\bullet\bullet})^{\bullet} + (Cu_{Nb}''' - V_O^{\bullet\bullet})' + O_2(g) + 2CO(g) + 2K_K^{\times} + 2Na_{Na}^{\times} + 2Nb_{Nb}^{\times} + 9O_O^{\times}. \quad (3)$$

CuO-doped KNN compounds thus exhibit a pronouncedly different defect structure as compared to doped PZT or $BaTiO_3$, for which it is well established that acceptor ions in general form *dimeric* defect complexes with an electric dipole moment;[30–33] *trimeric* complexes such as the $(V_O^{\bullet\bullet} - Cu_{Nb}''' - V_O^{\bullet\bullet})^{\bullet}$ that presumably exhibit mainly elastic distortions are absent in PZT and $BaTiO_3$. Furthermore, local differences in the nature of chemical bonding between the Cu^{2+}-functional center and its coordinated ions were recently reported.[34]

Because dimeric defect complexes were shown to reorient under an applied external field,[42] and assuming the trimeric might be reoriented under sufficiently strong field as well, the piezoelectric properties of CuO-doped KNN compounds can be interpreted on an atomic scale as follows: recently it has been reported that CuO-doped KNN exhibits markedly enhanced mechanical quality factors.[13–15] The interaction of the $(V_O^{\bullet\bullet} - Cu_{Nb}''' - V_O^{\bullet\bullet})^{\bullet}$ defect complex with two types of domain walls is schematically illustrated in Figure 5. In Figure 5(a), the ferroelectric strain is perpendicular to the defect-induced local strain on the right side of the domain wall. A movement of the domain wall to the left increases the elastic energy unless the defect complex rotates as depicted in Figure 5(a). This effect does not occur for the configuration depicted in Figure 5(b), where ferroelectric and defect-induced local strains are parallel on both sides of the domain wall. Owing to the reorientation of the $(V_O^{\bullet\bullet} - Cu_{Nb}''' - V_O^{\bullet\bullet})^{\bullet}$ defect complex, as described for the mechanism in Figure 5(a), the oxygen vacancies have to migrate around the Cu^{2+} functional center. Because this process involves a hopping of two oxygen vacancies a considerably high amount of energy is needed, such that an effective pinning of domain walls may be provided.[1]

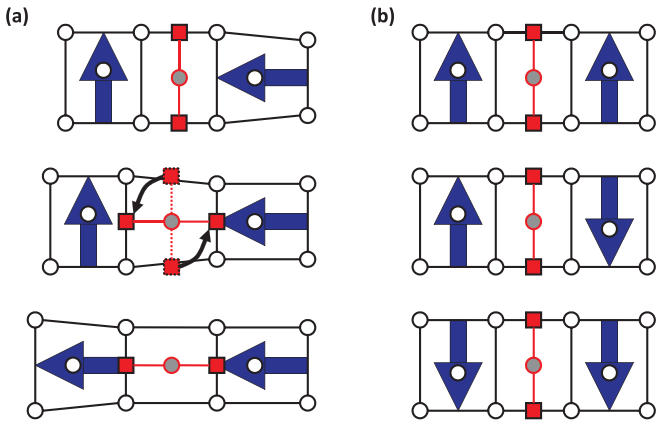

FIG. 5. Interaction between the $(V_O^{\bullet\bullet} - Cu_{Nb}''' - V_O^{\bullet\bullet})^{\bullet}$ defect complex with two types of domain walls. The orientation of spontaneous polarization is represented by a bold blue arrow. (a) Ferroelectric and defect-induced strain parallel on one side of the domain wall and perpendicular on the other. (b) Ferroelectric and defect-induced strain parallel on both sides of the domain wall.

In summary, "lead-free" piezoelectric sodium potassium niobate has been studied with respect to its defect structure when doping with CuO. The results indicate that two kinds of mutually compensating charged defect complexes are formed, $(Cu_{Nb}''' - V_O^{\bullet\bullet})'$ and $(V_O^{\bullet\bullet} - Cu_{Nb}''' - V_O^{\bullet\bullet})^{\bullet}$, similar to the situation for the pure members of the KNN solid solution system.[43,44] In particular, a trimeric defect complex has been identified that defines a point of departure to explore electromechanical properties in lead-free ferroelectrics. The trimeric $(V_O^{\bullet\bullet} - Cu_{Nb}''' - V_O^{\bullet\bullet})^{\bullet}$ defect complex primarily has an elastic dipole moment, whereas the dimeric $(Cu_{Nb}''' - V_O^{\bullet\bullet})'$ defect possesses an electric dipole moment in addition to an elastic distortion. Both types of defect complexes can impede domain-wall motion and may contribute to ferroelectric "*hardening*."

This research has been financially supported by the DFG through the projects EI 498/1-2, EL 155/21-2, and HO 1165/14-2.

[1]U. Robels and G. Arlt, J. Appl. Phys. **73**, 3454–3460 (1993).
[2]X. Ren, Nature Mater. **3**, 91–94 (2004).
[3]S. Pöykkö and D. J. Chadi, Phys. Rev. Lett. **83**, 1231–1234 (1999).
[4]J. F. Scott and M. Dawber, Appl. Phys. Lett. **76**, 3801–3803 (2000).
[5]L. E. Cross, Nature **432**, 24–25 (2004).
[6]J. Rödel, W. Jo, K. T. P. Seifert, E. M. Anton, T. Granzow, and D. Damjanovic, J. Am. Ceram. Soc. **92**, 1153–1177 (2009).
[7]R.-A. Eichel and H. Kungl, Funct. Mater. Lett. **3**, 1–4 (2010).
[8]D. Damjanovic, N. Klein, J. Li, and V. Porokhonskyy, Funct. Mater. Lett. **3**, 5–13 (2010).
[9]T. Takenaka and H. Nagata, J. Eur. Ceram. Soc. **25**, 2693–2700 (2005).
[10]M. Kosec, B. Malic, A. Bencan, T. Rojac, and J. Tellier, Funct. Mater. Lett. **3**, 15–18 (2010).
[11]Y. Saito, H. Takao, T. Tani, T. Nonoyama, K. Takatori, T. Homma, T. Nagaya, and M. Nakamura, Nature **432**, 84–87 (2004).
[12]R.-A. Eichel, P. Erhart, P. Träskelin, K. Albe, H. Kungl, and M. J. Hoffmann, Phys. Rev. Lett. **100**, 095504 (2008).
[13]M. Matsubara, T. Yamaguchi, K. Kikuta, and S. Hirano, Jpn. J. Appl. Phys. Part 1 **43**, 7159–7163 (2004).
[14]E. Li, H. Kakemoto, S. Wada, and T. Tsurumi, IEEE Trans. Ultrason. Ferroelectr. Freq. Control **55**, 980–987 (2008).
[15]F. Azough, M. Wegrzyn, R. Freer, S. Sharma, and D. Hall, J. Eur. Ceram. Soc. **31**, 569–576 (2011).
[16]R.-A. Eichel, J. Am. Ceram. Soc. **91**, 691–701 (2008).
[17]R.-A. Eichel, H. Kungl, and P. Jakes, Mater. Technol. (2013) doi:10.1179/175355513X13715615193120.
[18]S. Körbel, P. Marton, and C. Elsässer, Phys. Rev. B **81**, 174115 (2010).
[19]S. Körbel, "Atomistic modeling of Cu doping in the lead-free ferroelectric potassium sodium niobate," PhD dissertation, http://www.freidok.uni-freiburg.de/volltexte/8860.
[20]S. Körbel and C. Elsässer, "Alignment of ferroelectric polarization and defect complexes in copper-doped potassium niobate," Phys. Rev. B (submitted).
[21]R.-A. Eichel, M. D. Drahus, P. Jakes, E. Erünal, E. Erdem, S. K. S. Parashar, H. Kungl, and M. J. Hoffmann, Mol. Phys. **107**, 1981–1986 (2009).
[22]Z. Feng and X. Ren, Phys. Rev. B **77**, 134115 (2008).
[23]E. Aksel, E. Erdem, P. Jakes, J. L. Jones, and R.-A. Eichel, Appl. Phys. Lett. **97**, 012903 (2010).
[24]E. Erdem, R.-A. Eichel, H. Kungl, M. J. Hoffmann, A. Ozarowski, J. van Tol, and L. C. Brunel, Phys. Scr. T **129**, 12–16 (2007).
[25]P. Jakes, E. Erdem, R.-A. Eichel, L. Jin, and D. Damjanovic, Appl. Phys. Lett. **98**, 072907 (2011).
[26]E. Erdem, P. Jakes, S. K. S. Parashar, K. Kiraz, M. Somer, A. Rüdiger, and R.-A. Eichel, J. Phys.: Condens. Matter **22**, 345901 (2010) .
[27]E. Aksel, P. Jakes, E. Erdem, D. M. Smyth, A. Ozarowski, J. van Tol, J. L. Jones, and R.-A. Eichel, J. Am. Ceram. Soc. **94**, 1363–1367 (2011).
[28]M. D. Drahus, P. Jakes, E. Erdem, and R.-A. Eichel, Solid State Ionics **184**, 47–51 (2011).

[29]D. M. Smyth, *The Defect Chemistry of Metal Oxides* (Oxford University Press, New York, 2000).
[30]K. A. Müller, W. Berlinger, and J. Albers, Phys. Rev. B **32**, 5837 (1985).
[31]W. L. Warren, G. E. Pike, K. Vanheusden, D. Dimos, B. A. Tuttle, and J. Robertson, J. Appl. Phys. **79**, 9250 (1996).
[32]H. Meštrić, R.-A. Eichel, T. Kloss, K.-P. Dinse, So. Laubach, St. Laubach, and P. C. Schmidt, Phys. Rev. B **71**, 134109 (2005).
[33]E. Erdem, P. Jakes, R.-A. Eichel, D. C. Sinclair, M. Pasha, and I. M. Reaney, Funct. Mater. Lett. **3**, 65–68 (2010).
[34]R.-A. Eichel, E. Erünal, M. D. Drahus, D. M. Smyth, J. van Tol, J. Acker, H. Kungl, and M. J. Hoffmann, Phys. Chem. Chem. Phys. **11**, 8698–8705 (2009).
[35]J. Acker, H. Kungl, and M. J. Hoffmann, J. Am. Ceram. Soc. **93**, 1270–1281 (2010).
[36]J. Acker, H. Kungl, and M. J. Hoffmann, J. Eur. Ceram. Soc. **33**, 2127–2139 (2013).
[37]P. Erhart and K. Albe, J. Appl. Phys. **102**, 084111 (2007).
[38]C. Elsässer, N. Takeuchi, K. M. Ho, C. T. Chan, P. Braun, and M. Fähnle, J. Phys. Condens. Matter **2**, 4371 (1990).
[39]F. Lechermann, F. Welsch, C. Elsässer, C. Ederer, M. Fähnle, J. M. Sanchez, and B. Meyer, Phys. Rev. B **65**, 132104 (2002).
[40]N. J. Ramer and A. M. Rappe, J. Phys. Chem. Sol. **61**, 315 (2000).
[41]L. Bellaiche and D. Vanderbilt, Phys. Rev. B **61**, 7877 (2000).
[42]L. X. Zhang, E. Erdem, X. Ren, and R.-A. Eichel, Appl. Phys. Lett. **93**, 202901 (2008).
[43]E. Erünal, R.-A. Eichel, S. Körbel, C. Elsässer, J. Acker, H. Kungl, and M. J. Hoffmann, Funct. Mater. Lett. **3**, 19–24 (2010).
[44]E. Erünal, P. Jakes, S. Körbel, J. Acker, H. Kungl, C. Elsässer, M. J. Hoffmann, and R.-A. Eichel, Phys. Rev. B **84**, 184113 (2011).